EARTHQUAKE OBSERVATIONS AT A 35,000kl LNG TANK

by Nobuhiko Sato,[I]
Tsuneo Katayama [II] and
Keizaburo Kubo[III]

SYNOPSIS

Results of earthquake observations made at the site of a 35,000kl liquid natural gas tank are reported. Earthquake records analyzed include accelerations on the tank foundation slab as well as those on the surface of and in the surrounding ground. By using autocorrelation functions, power spectral densities and frequency response functions of four of the better acceleration records, frequency characteristics were investigated for the tank foundation slab, the surrounding surface layer and earthquake motions in the mud stone layer which underlies the site. The amplification factors of maximum accelerations from baserock motions to ground surface and tank slab motions were also investigated.

[I]Research Assistant, [II]Associate Professor and [III]Professor of the Institute of Industrial Science, University of Tokyo.

TANK AND SITE CONDITIONS

The liquid natural gas (LNG) tank No. 3 of the Negishi Factory, in Yokohama, of the Tokyo Gas Company is about 40m in both diameter and height and has a storage capacity of 35,000kl (Fig. 1). The total weight of the tank and LNG amounts to 21,440t. The tank is bolted to an 80cm-thick reinforced concrete circular foundation slab which is supported by 341 steel tube piles (Fig. 2).

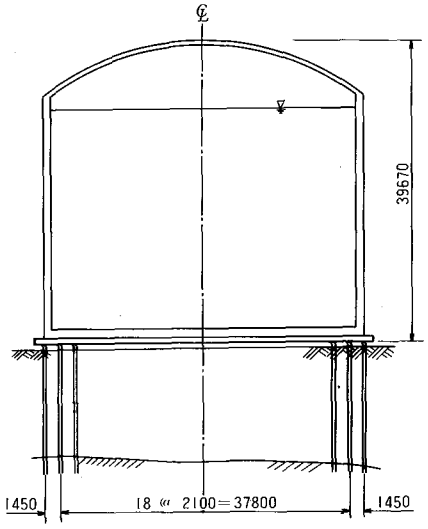

Fig. 1 LNG Tank

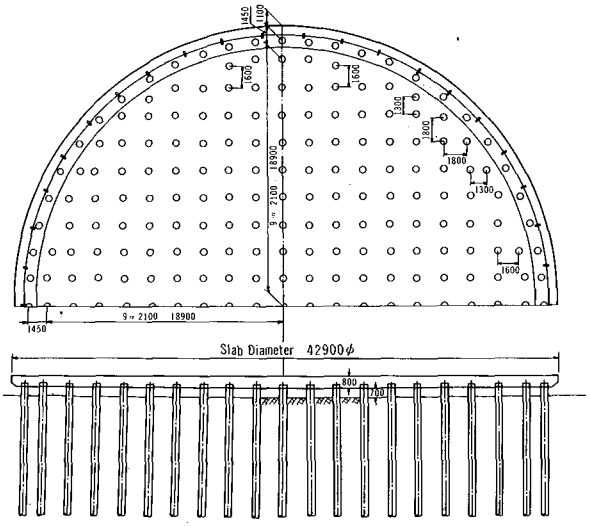

Fig. 2 Layout of Steel Tube Piles

The steel tube pile is 508mm in outer diameter and has a thickness of 12.7mm except for the upper 4m portion for which the thickness is 16mm. As seen from Fig. 3, the pile head is anchored into the foundation slab for a length of 40cm.

There is a clearance of about 70cm between the foundation slab and the ground surface.

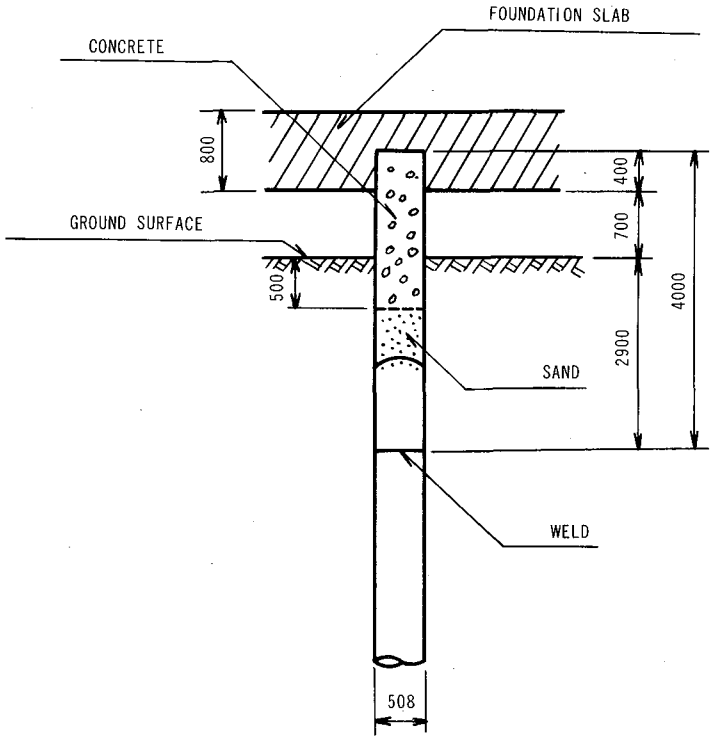

Fig. 3 Detail of Pile Head

Use of vertical sand drains and preloading by sand surcharge of 3.5m had been made for the site in order to improve the engineering performances of the soil to a depth of 10m. Typical subsoil profiles are shown in Fig. 4 for the two points under the tank. The site is covered with recently-filled loose sandy soils to a depth of about 5m. The alluvial layer beneath it is generally composed of two parts, the upper silty soils and the lower sandy soils. Standard N values were found to be 1 to 2 for the former and 5 to 8 for the latter. The hard mud stone layer, called Dotan in Japanese, with N values greater than 50 was found to exist at depths varying between 10 and 30m. Supporting steel piles were driven into this mud stone layer for a length of at least 50cm. From pile driving data for the foundations of the tank and piping systems, it was possible to estimate the variations of the depth to the mud stone layer. Fig. 5 shows such variations along three lines. It is noted that the inclination of the mud stone layer is steep in the E-W direction.

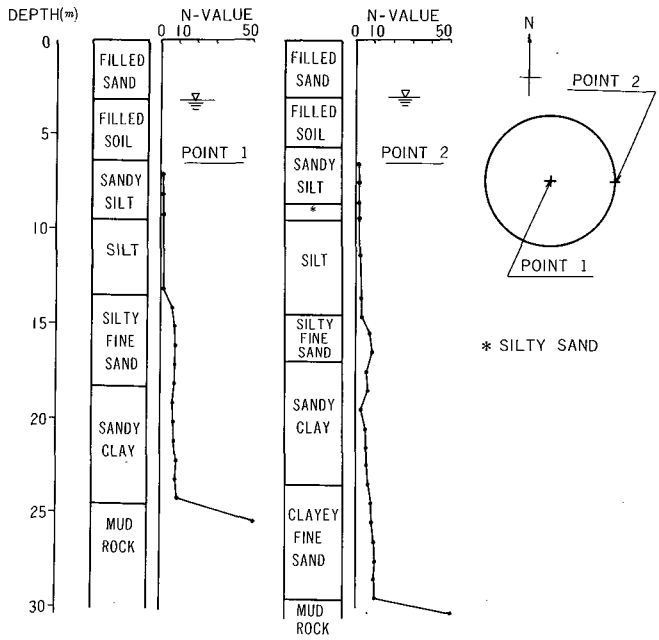

Fig. 4 Typical Subsoil Profiles

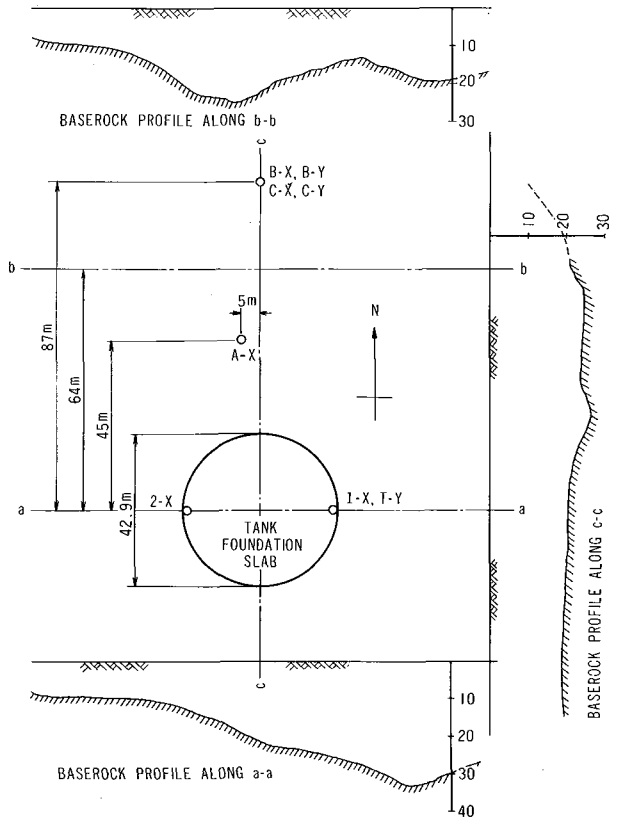

Fig. 5 Locations of Seismometers and Depth Variations of Mud Stone Layer

INSTRUMENTATION AND EARTHQUAKE RECORDS

A total of eight acceleration-type seismometers with the maximum sensitivity of 10μA/gal were installed for earthquake observations. The signal obtained by a seismometer is amplified and fed to an oscillograph to be recorded on a photosensitized paper. The overall measurement system was found to give a flat response over a frequency range between 0.4 and 20 Hz. The locations and directions of seismometers are shown in Fig. 5 and Table 1 with respective code names used hereafter. There are two seismometers C-X and C-Y installed at about 10m from the ground surface in the mud stone layer, three seismometers A-X, B-X, and B-Y on the ground surface, and three seismometers 1-X, 2-X, and T-Y on the foundation slab of the tank. Seismometers 1-X and 2-X were installed because the movements of the slab in the N-S direction were expected to differ in magnitude due to the steep inclination of the mud stone layer in the E-W direction. Wave forms recorded by 1-X and 2-X were synthesized to obtain.

$$T\text{-}X = ((1\text{-}X) + (2\text{-}X))/2$$

and

$$T\text{-}R = ((1\text{-}X) - (2\text{-}X))/2,$$

the latter of which divided by the radius of the tank gives the angular acceleration $\ddot{\Theta}$ (rotational component) of the slab motion (Fig. 6). It should be noted that records in the mud stone layer are not obtained directly below the tank but at a place about 90m distant from the center of the tank because boring was prohibited near the tank.

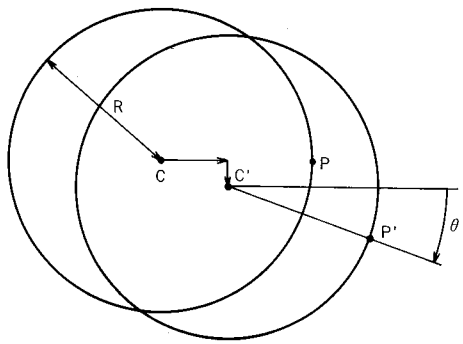

Fig. 6 Horizontal Motion of Tank Slab

Observations began in October, 1972, and about 20 earthquakes had been recorded as of September, 1973. Some earthquake records are very small in amplitude and could not be digitized. For such records only maximum acceleration values could be used for analysis. Six records were digitized at 0.05 seconds intervals and detailed studies were made with respect to their characteristics in the frequency domain. Even for these records complete data could not be utilized because several of the oscillogram

traces were not obtained due to the instrumental malfunction or they are too small to make accurate digitization. Two examples of recorded accelerations are shown in Figs. 7(a) and (b). Most of the present analysis will be made by using four of the six digitized motions as shown in Table 2.

Since, in order to accumulate as many records as possible, the amplifiers and the oscillograph were set so that even small earthquakes could be recorded, moderate earthquakes as listed in Table 2 yielded acceleration peaks which were too big to stay on scale. This also made some of the oscillogram traces during the most intensive shaking undistinguishable each other. Therefore, the portions of accelerograms used for analysis did not always coincide with those of the strongest shaking. It is intended that, after a number of small earthquake records have been obtained, the sensitivity of the measuring system will be lowered to record strong shakings without loss of large acceleration peaks.

Table 1 Locations of Seismometers (refer to Fig. 5)

Code Name	Direction	Location	Depth to Baserock
1-X	N-S	On the eastern edge of the slab	26m
2-X	N-S	On the western edge of the slab	12m
T-Y	E-W	On the eastern edge of the slab	26m
A-X	N-S	On the ground surface, about 45m to the north from the center of the slab	20m
B-X	N-S	On the ground surface, about 87m to the north from the center of the slab	10m
B-Y	E-W	ditto	ditto
C-X	N-S	In the mud stone layer, about 10m deep from the ground surface and about 87m to the north from the center of the slab	--
C-Y	E-W	ditto	--

Table 2 Four Earthquakes Used for Analysis

Earthquake Number	Date of Occurrence	Epicenter		Focal Depth	Magni-tude	Epicentral Distance
		N	E			
4	Dec.4,1972	33°12'	141°05'	50km	7.3	280km
5	Between Dec. 4 and 8, 1972	Probably one of the aftershocks of Earthquake No. 4				
6	Dec.8,1972	35°35'	140°00'	90km	?	38km
20	March 27, 1973	35°30'	139°48'	60km	?	18km

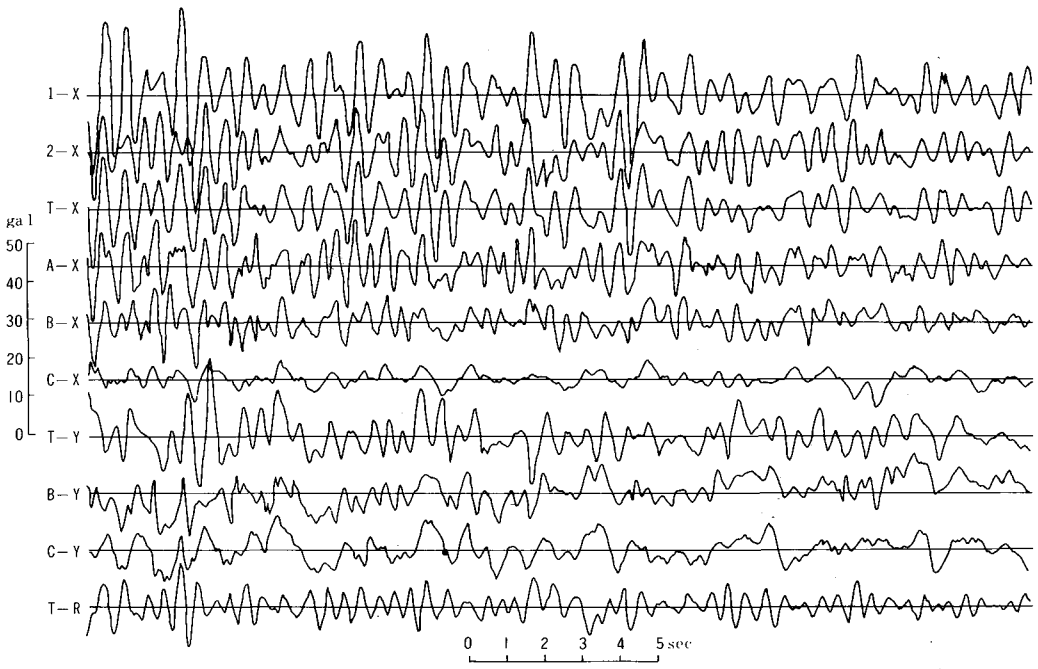

Fig. 7(a) Example of Earthquake Records --- Earthquake No. 4

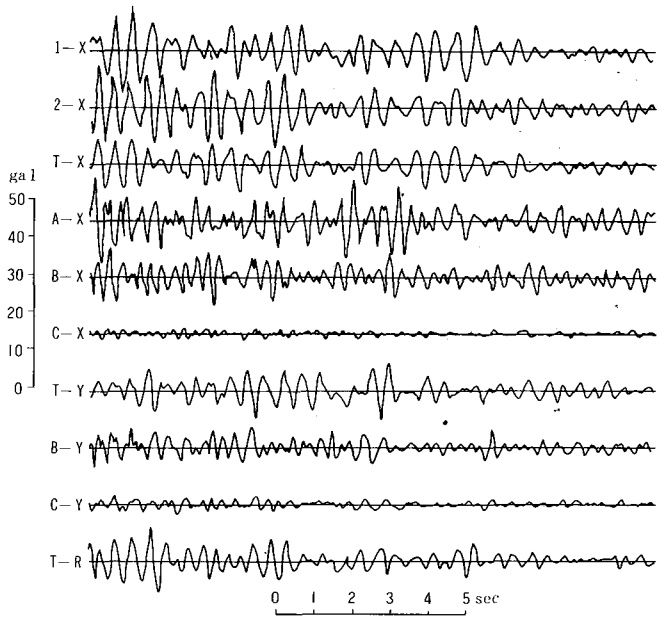

Fig. 7(b) Example of Earthquake Records --- Earthquake No. 6

RESULTS OF ANALYSIS AND DISCUSSIONS

Autocorrelation functions and power spectral densities were calculated from the digitized records of the four earthquake motions previously mentioned. As an example, the results for earthquake No. 6 are shown in Fig. 8. The values of frequencies which correspond to the highest peaks of power spectral densities are summarized in Table 3 together with the predominant frequencies as estimated from autocorrelation functions.

Frequency Characteristics of Earthquake Motions in Mud Stone Layer Power spectral densities of the N-S components of the four earthquake motions recorded in the mud stone layer are shown in Fig. 9. As seen from Table 2, the epicentral distances of earthquakes No. 4 and No. 5 were relatively large, while records No. 6 and No. 20 were obtained from near earthquakes. It seems that, for earthquakes with long epicentral distances, waves with low frequencies predominate in the motions recorded in the mud stone layer, whereas earthquakes with short epicentral distances produce baserock motions with higher frequencies. Figs. 10(a) and (b) show power spectral distributions of the N-S and the E-W components of baserock motions for the four earthquakes. It may be seen that frequency characteristics of the N-S and the E-W motions are very similar for all of the four records analyzed. Fig. 10 clearly shows that frequencies of baserock motions caused by far earthquakes are mostly limited below 3Hz and that baserock motions of near earthquakes have most of their power in the frequency range between 1 and 6Hz.

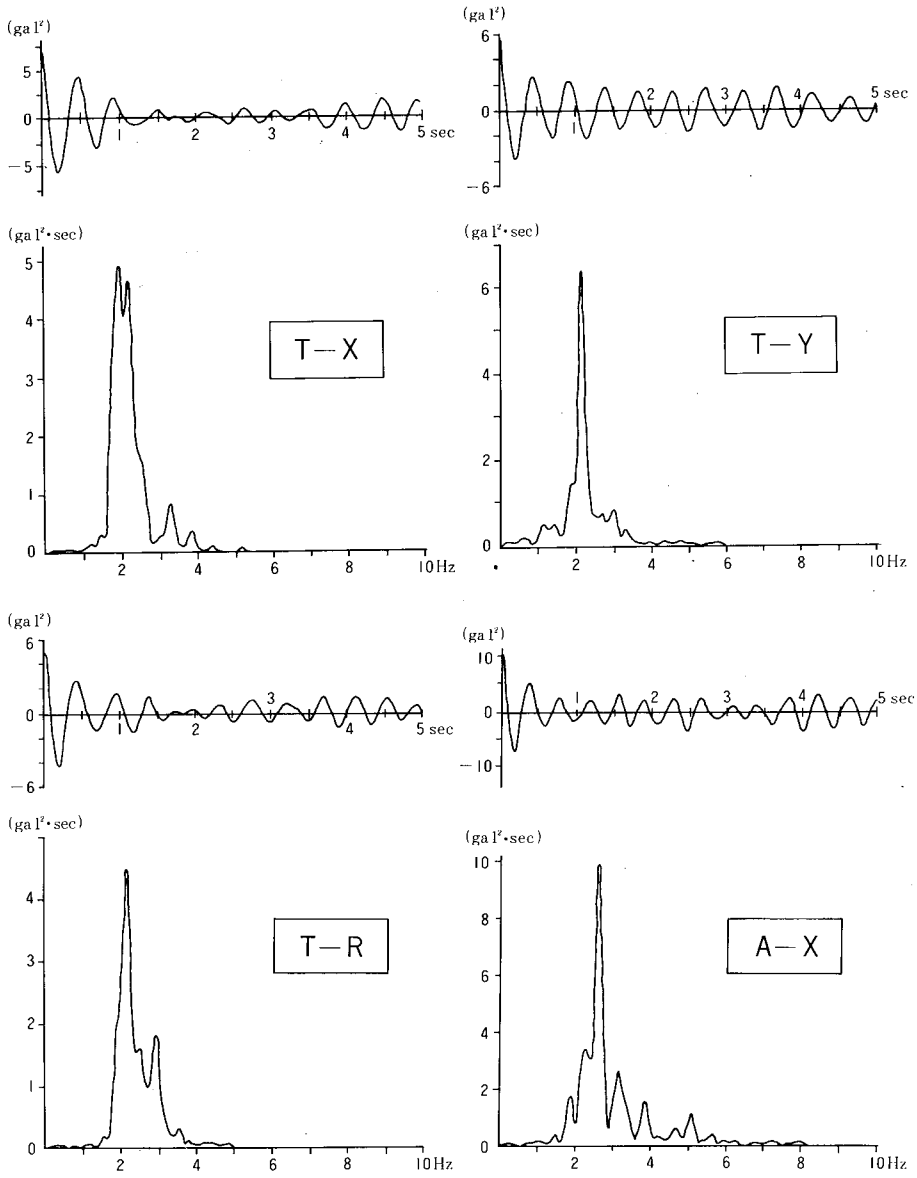

Fig. 8 Autocorrelation Functions and Power Spectral Densities for Earthquake Record No. 6

Frequency Characteristics of Ground Surface Motions In order to investigate the effects of soft surface layers on the frequency characteristics of earthquake motions on the ground surface, frequency response functions H(f) were computed by using the following relationship,

$$H(f) = \left[\frac{S_{surface}(f)}{S_{base}(f)}\right]^{\frac{1}{2}}$$

in which $S_{surface}(f)$ and $S_{base}(f)$ are the power spectral densities of earthquake motions recorded on the ground surface and in the mud stone layer, respectively.

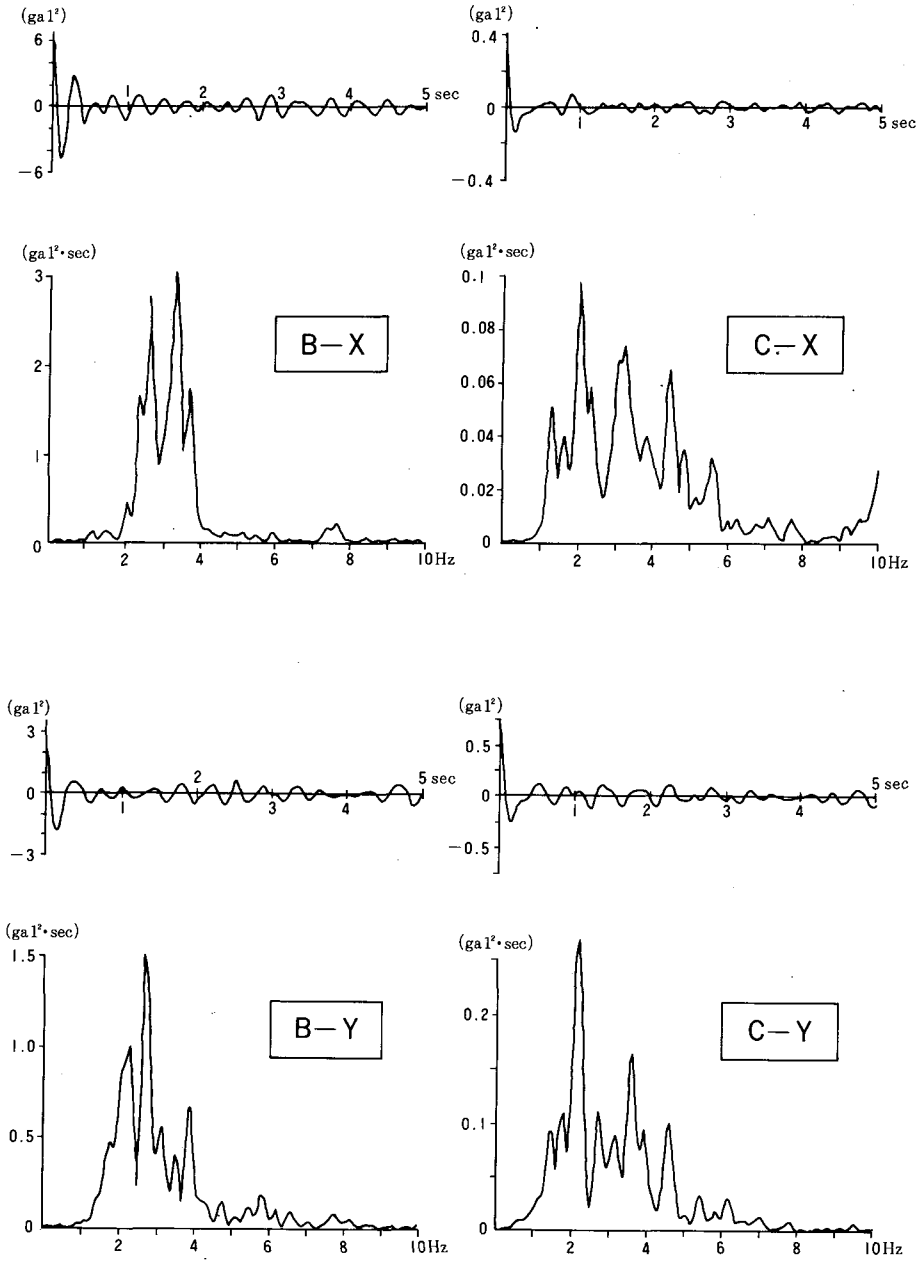

Fig. 8 Autocorrelation Functions and Power Spectral Densities for Earthquake Record No. 6

Table 3 Summary of Predominant Frequencies Obtained from Power Spectral Densities (PSD) and Autocorrelation Functions (ACF)

		Earthquake No.4		Earthquake No.5		Earthquake No.6		Earthquake No.20	
		PSD	ACF	PSD	ACF	PSD	ACF	PSD	ACF
On Tank Slab	T-X	1.7Hz	1.7Hz	1.7Hz	1.7Hz	2.0Hz	2.1Hz	1.8Hz	1.8Hz
	T-Y	2.0Hz	2.0Hz	0.3Hz	---	2.2Hz	2.2Hz	1.8Hz	1.8Hz
	T-R	2.1Hz	2.1Hz	1.8Hz	1.8Hz	2.2Hz	2.1Hz	2.7Hz	2.7Hz
On Ground Surface	A-X	1.5Hz (2.3Hz)	---	0.5Hz	---	2.6Hz	2.6Hz	2.7Hz	2.6Hz
	B-X	2.3Hz	2.3Hz	0.5Hz	0.5Hz	3.4Hz (2.7Hz)	3.1Hz	2.9Hz (2.6Hz)	2.5Hz
	B-Y	0.2Hz	---	0.3Hz	---	2.7Hz	---	---	---
In Mud Stone Layer	C-X	0.3Hz (0.6Hz)	---	0.5Hz	0.5Hz	2.1Hz	---	3.1Hz	---
	C-Y	0.2Hz (0.5Hz)	---	0.3Hz	---	2.2Hz	---	2.0Hz (4.3Hz)	---

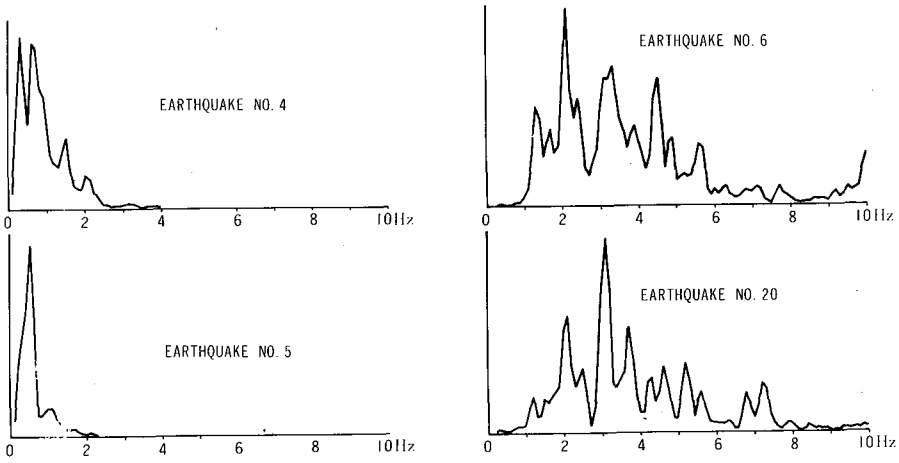

Fig. 9 Power Spectral Densities of N-S Motions in Mud Stone Layer

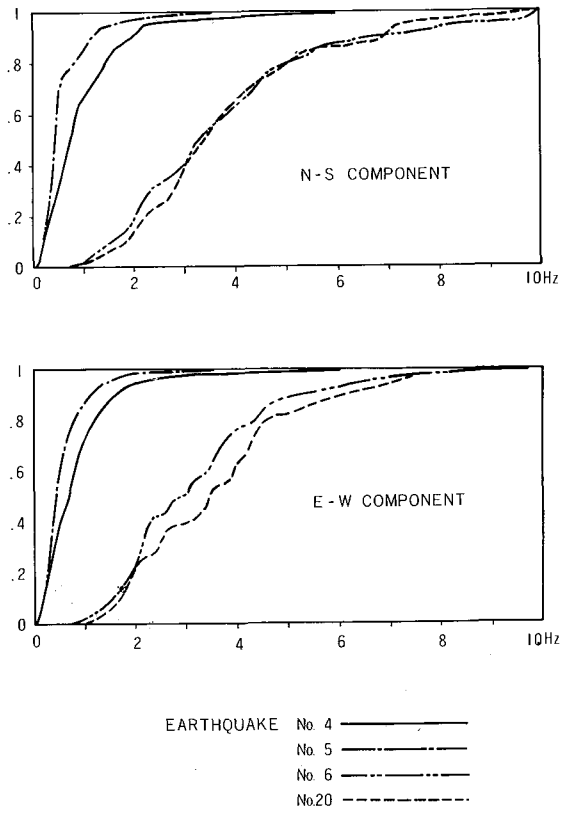

Fig. 10 Power Spectral Distributions of Earthquake Motions in Mud Stone Layer

Results are shown in Figs. 11, 12, and 13. Frequencies corresponding to the highest peaks and their ordinate values are summarized in Table 4. As seen from Figs. 11 and 12, the highest peaks of the frequency response functions for the N-S direction are located between 2.5Hz and 2.8Hz. Fig. 13 shows that the highest peaks for the E-W direction are not so distinguished as those for the N-S direction. However, they are also found somewhere between 2.5Hz and 3.0Hz. Hence, it seems reasonable to conclude that the predominant frequency of the surface layer of the site lies between 2.5 and 3.0Hz, irrespective of direction. By considering the fact that the depths to the mud stone layer at point A and B are about 20m and 10m, respectively, the results shown above indicate that the predominant frequency of a site cannot be simply estimated from the thickness of the surface layer but the three-dimensional formation of the layer must be taken into account. The peak values of frequency response functions in Table 4 clearly show that the magnification of acceleration at the predominant frequency is greater at point A where the thickness of surface layer is about 20m than that at point B with the surface layer thickness of 10m.

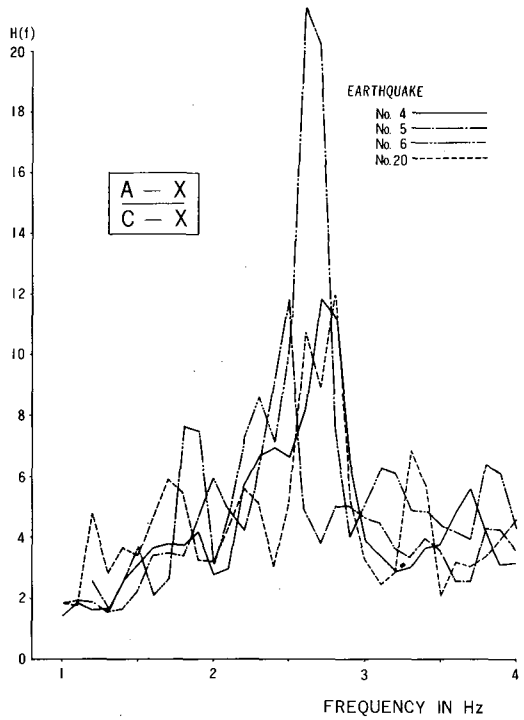

Fig. 11 Frequency Response Functions Obtained from N-S Surface Motions at Point A

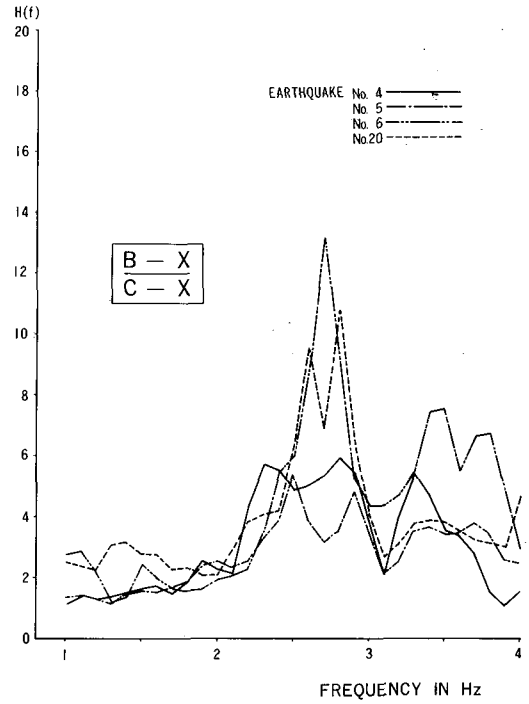

Fig. 12 Frequency Response Functions Obtained from N-S Surface Motions at Point B

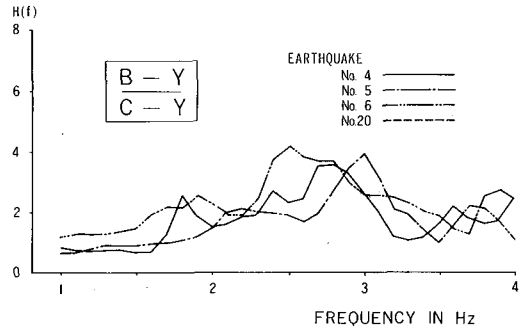

Fig. 13 Frequency Response Functions Obtained from E-W Surface Motions at Point B

Frequency Characteristics of Tank Foundation Slab Frequency response functions of the tank foundation slab relative to the baserock and the ground surface motions were calculated from respective power spectral densities and are shown in Figs. 14, 15, and 16. Frequencies and values of H(f) corresponding to the highest peaks are summarized in Table 5. From Fig. 14 and Table 5, the fundamental frequency of the tank foundation slab in the N-S translational motion can be estimated as 1.8 ∿ 1.9Hz. Similar frequencies can also be observed from Fig. 15 which shows the frequency response function of the foundation slab relative to the ground surface motions at point A. However, the fact that

the magnitude of amplification shown in Fig. 15 is generally much smaller than that in Fig. 14 indicates that the motion of the foundation slab during earthquakes is mostly governed by the motion of the surrounding surface layer.

As can be seen from Fig. 16, the frequency response functions of the E-W translational motions of the foundation slab relative to the E-W baserock motions do not show clearly-defined peaks. This is probably due to the fact that the mud stone layer has a steep inclination in the E-W direction as shown in Fig. 5. The fundamental frequency of the slab in the E-W direction seems to be a little higher than that in the N-S direction.

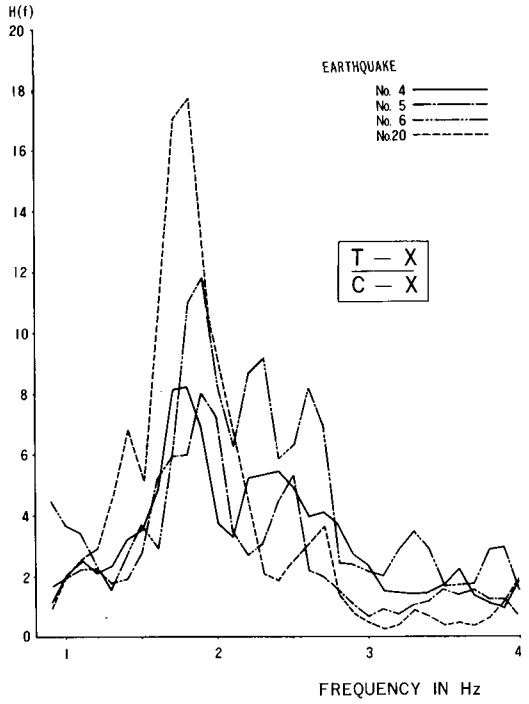

Fig. 14 Frequency Response Functions of Tank Slab in N-S Direction Relative to Baserock Motions

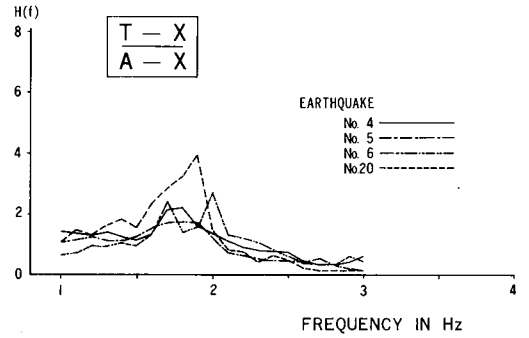

Fig. 15 Frequency Response Functions of Tank Slab in N-S Direction Relative to Ground Surface Motions at Point A

Table 4 Highest Peaks of Frequency Response Functions for Surface Layer

		Earthquake No.4	Earthquake No.5	Earthquake No.6	Earthquake No.20
A-X / C-X	f^*_{max}	2.7	2.5	2.6	2.8
	$H(f_{max})$**	11.5	11.8	21.5	12.0
B-X / C-X	f_{max}	2.8	2.5	2.7	2.8
	$H(f_{max})$	5.9	5.4	13.2	10.9
B-Y / C-Y	f_{max}	2.8	3.0	2.5	---
	$H(f_{max})$	3.6	3.9	4.2	---

* f_{max} = frequency corresponding to highest peak in Hz

**$H(f_{max})$ = value of frequency response function at f_{max}

Table 5 Highest Peaks of Frequency Response Functions for Tank Foundation Slab

		Earthquake No.4	Earthquake No.5	Earthquake No.6	Earthquake No.20
T-X / C-X	f^*_{max}	1.8	1.9	1.9	1.8
	$H(f_{max})$**	8.2	8.0	11.7	17.7
T-Y / C-Y	f_{max}	2.1	2.1	2.5	1.8
	$H(f_{max})$	4.6	3.6	6.9	5.4
T-X / A-X	f_{max}	1.8	1.8	2.0	1.9
	$H(f_{max})$	2.2	1.7	2.7	3.9

* f_{max} = frequency corresponding to highest peak in Hz

**$H(f_{max})$ = value of frequency response function at f_{max}

Ratios of Maximum Acceleration Responses Fig. 17 shows the ratios of maximum acceleration response values of the ground surface motions to those of the motions in the mud stone layer. It is seen that the ratios at point A where the surface layer thickness is about 20m are generally greater than those at point B with the surface layer thickness of 10m. For small maximum accelerations from the mud stone layer, the values at point A generally lie between 4 and 7, and those at point B between 1.5 and 4. Consequently, there is an average factor of about 2 between the maximum acceleration responses at these two points.

The ratios between the maximum slab accelerations and the maximum baserock accelerations are shown in Fig. 18, from which it is found that the ratio is greater for the motions in the N-S direction. This also indicates that the steep slope of the mud stone layer in the E-W direction reduces the acceleration amplification of the slab in this direction. It may be said that, generally speking, values of the ratios for the tank are of the same order as those for the surface motions. Though the maximum accelerations of most of the records so far obtained are very small as seen from Figs. 17 and 18, there seems to be a tendency for the acceleration amplification ratio to decrease with the increase of the baserock acceleration.

Fig. 19 shows the maximum acceleration amplification ratios between the tank slab and the ground surface at point A in the N-S direction. By comparing the values in Fig. 19 with those in Fig. 18, it may be concluded that the motion of the tank foundation slab is mainly affected by the movement of the surrounding surface layer during earthquakes.

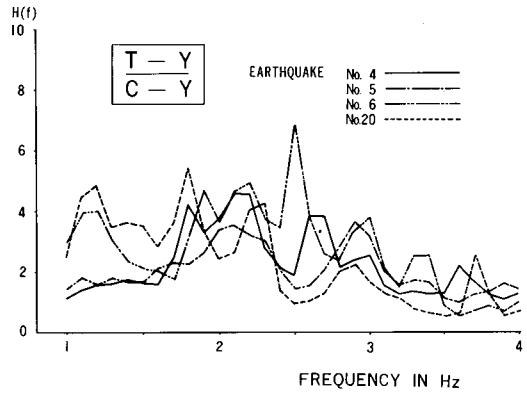

Fig. 16 Frequency Response Functions of Tank Slab in E-W Direction Relative to Baserock Motions

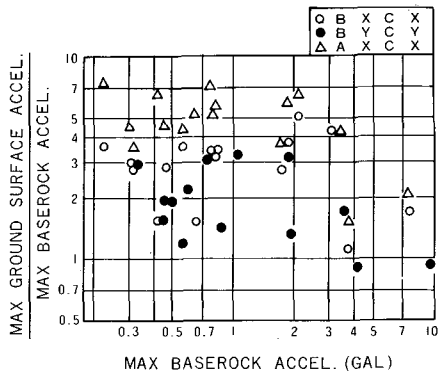

Fig. 17 Ratios Between Maximum Ground Surface Accelerations and Maximum Baserock Accelerations

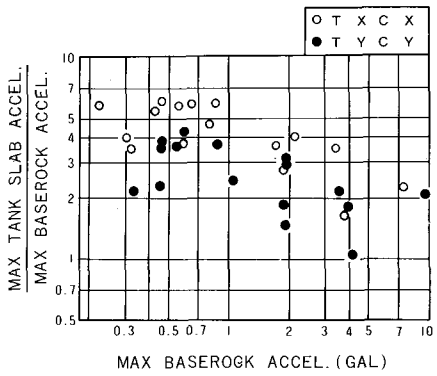

Fig. 18 Ratios Between Maximum Slab Accelerations and Maximum Baserock Accelerations

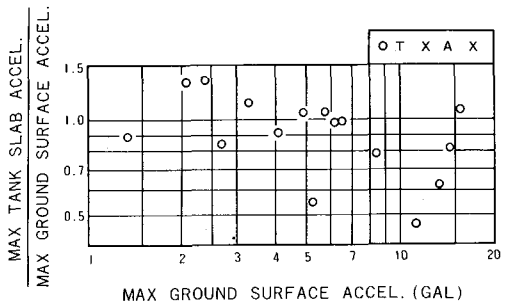

Fig. 19 Ratios Between Maximum Slab Accelerations and Maximum Ground Surface Accelerations at Point A

CONCLUDING REMARKS

From the analysis of the earthquake records obtained on the foundation slab of a 35,000kl LNG tank and at several locations on the ground surface and in the ground of the tank site, the following findings have been made:

1) Frequencies of earthquake motions in the mud stone layer caused by far earthquakes (Δ>200km, say) are limited below 3Hz, whereas baserock motions of near earthquakes (Δ<50km) have most of their power in the frequency range between 1 and 6Hz.

2) The fundamental frequency of the surface layer of the site was found to be between 2.5 and 3.0Hz, irrespective of direction and depth to the mud stone layer. This seems to indicate that it is important to take into account the three-dimensional formation of the surface layer in order to estimate the predominant frequency of a site.

3) The lowest translational motion of the tank foundation slab was found to have a frequency between 1.8 and 1.9Hz. The motion of the slab was found to be largely influenced by the movement of the surrounding surface layer. Difference in the acceleration amplifications of the N-S and the E-W directions indicates that the slope of the mud stone layer supporting foundation piles gives a substantial influence on the dynamic behaviors of the slab during earthquakes.

4) For earthquake motions with small maximum accelerations in the mud stone layer (a_{max} < 3gal), the ratios between the maximum ground surface accelerations and the maximum baserock accelerations vary from 1.5 to 4 for a surface layer thickness of 10m, and from 4 to 7 for a surface layer thickness of 20m.

In addition to further examinations of recorded earthquake motions, studies are presently being made on the evaluation of the dynamic properties of the pile foundations by means of analytical as well as observational approach.

ACKNOWLEDGMENT

The authors would like to express their appreciation to the Tokyo Gas Company and the Tokyo Electricity Company for permitting earthquake observations, and to Messrs. K. Itoh and Y. Masui for the preparation of observational results and the drawing of figures in this paper.